Permeability of saturated and unsaturated iron ore fines

H. WANG [i], J. KOSEKI[ii] and T. NISHIMURA[iii]

i) Assistant Professor, Waseda Research Institute for Science and Engineering, Waseda University, 3-4-1 Ohkubo, Shinjuku-ku, Tokyo 169-8555, Japan
ii) Professor, Department of Civil Engineering, The University of Tokyo, 7-3-1 Hongo, Bunkyo-ku, Tokyo 113-0033, Japan
iii) Professor, Division of Architecture and Civil Engineering, Ashikaga University, 286-1 Omae-cho, Ashikaga-shi Tochigi 326-8558, Japan

ABSTRACT

Concerning on the liquefaction behavior of a type of bulk cargoes, iron ore fines (IOF), during maritime time transportation, systematic experimental and numerical programs were conducted. In this study, as an important parameter for seepage analysis, permeability of saturated and unsaturated typical IOF were evaluated in a triaxial system. As a comparison, similar tests were also conducted on a widely used laboratory material, Toyoura sand. The tests were conducted very carefully considering effects of system head loss and filter clogging issues on the hydraulic gradient applied to specimens. It was revealed that coefficient of permeability (k) of the typical IOF with compaction degree of 91-93% was about 1×10^{-5}m/s for saturated condition (S_r=100%) and 2×10^{-7} m/s for S_r=84%. In addition, k of IOF-B in a full S_r range was estimated based on water retention data and k of unsaturated Toyoura sand in the past studied were summarized, which suggested that the testing system performed reasonably well.

Keywords: Iron ore fines, permeability, triaxial system, liquefaction, Toyoura sand

1 INTRODUCTION

In 2009, casualties of two vessels loaded iron ore fines (IOF, a type of bulk cargoes transported at sea for the iron making industry) happened near Indian ports (IMO 2010a and 2010b). The casualties were reportedly caused by liquefaction of IOF due to its high water content when being loaded to the vessels in the monsoon season. For cargoes that are prone to liquefy, their transportable moisture limit (TML) is required to be determined by shippers before loading, and cargoes are not allowed to be loaded when their water content exceeds TML as stipulated in the International Maritime Solid Bulk Cargoes Code (IMSBC Code). Unfortunately, since there was not a specific instruction in IMSBC Code for IOF before the two casualties and some shippers treated IOF as un-liquefiable cargo (IOM 2010b, IMSBC 2012). To build an instruction for IOF, a series of studies were conducted by an iron ore technical working group (TWG) under the supervision of International Maritime Organization (IOM). Through these researches (IOM 2013b, 2013c, 2013d, 2013e and 2013f), TWG developed a new test method, modified Proctor-Fagerberg test (MPFT) for determination of TML of IOF, and this method has mandatorily been applied to IOF cargo contains both (1) 10% or more of fine particles less than 1 mm, and (2) 50% or more of particles less than 10 mm (IOM 2013a, IMO 2015). The MPFT is essentially the same as Proctor test but with smaller compaction energy and TML can be determined in the way as shown in Fig. 1 (note that gross water content =mass of water / (mass of IOF+ mass of water)). However, only a few studies were published on the evaluation of geotechnical behaviors of IOF as well as the liquefaction potential of IOF heap under nautical conditions except TWG works. Wang et al. (2014, 2016a, 2016b and 2018) revealed behaviors of IOF with saturated and unsaturated conditions under monotonic triaxial loading and cyclic loading, water retention properties etc. Wang et al. (2017 a), Chen et al. (2018) and Munro and Mohajerani (2018) conducted some numerical works, which indicate IOF heap may have high liquefaction or instability potential.

After loading unsaturated IOF to the vessel, due to the seepage during a voyage, saturated and unsaturated zones may form as schematically illustrated in Fig. 2. When the heap experience a cyclic motion induced by ocean wave or engine vibration during a voyage, liquefaction may be triggered especially for the saturated zone, which suggests that seepage analysis is very important for proper evaluation of IOF heap behaviors. In this study, permeability of IOF obtained by patient testing works were presented which provide basic information for seepage analysis in the IOF heap.

https://doi.org/10.3208/jgssp.v07.064

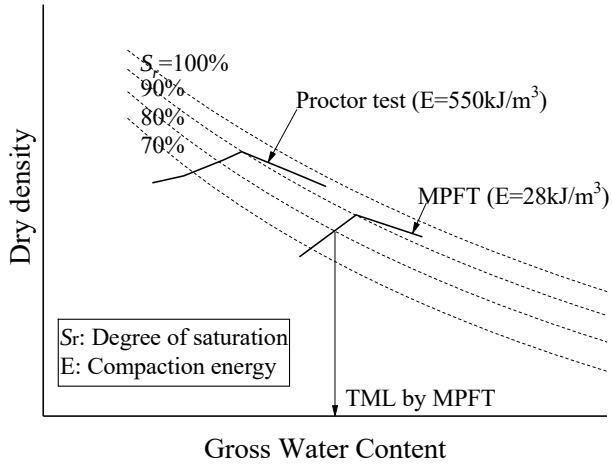

Fig. 1 Schematic illustration of method to determine TML

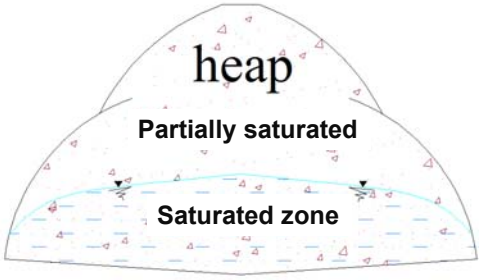

Fig. 2 Illustration of water distribution in IOF heap

2 TEST MATERIALS

A typical IOF, IOF-B and a widely used fine sand. Toyoura sand were used in this study. The specific gravity (G_s) values are 4.444 and 2.652, and fines contents (F_c) are 23.6 % and 0.1 % for IOF-B and Toyoura sand, respectively. Their gradation curves are shown in Fig. 3. The maximum dry density (ρ_{dmax}) and optimum water content (w_{opt}) are 2.79 Mg/m^3 and 12.0 % for IOF-B, respectively according to JIS (2009a) standard A1210. And the maximum and minimum void ratios (e_{max} and e_{min}) are 0.989 and 0.661 for Toyoura sand, respectively based on JIS (2009b) standard A1224.

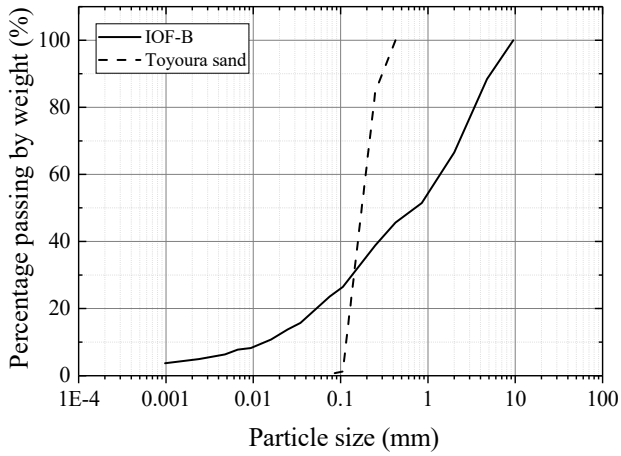

Fig. 3 Gradation curves of materials used

3 PREPARATIONS AND PROCEDURES

Permeability tests were conducted in a modified triaxial system as shown in Fig. 4 (for details: Wang et al. 2016c, 2017b and 2017c). It consisted of mainly four parts, the main body of the apparatus, water supply end, water receiver end and loading system (not shown). A double-tank system at the water supply end and a double-pipe system at the water receiver end were designed supplying a constant water head (H_{su}). A differential pressure transducer (DPT, see Fig. 4) was installed to measure the water head (H_m). Note that neither H_{su} nor H_m is not water head applied to the two ends of the specimen (H_{sp}) as illustrated in Section 4. It is worth mentioning that there is a coarse membrane filter glued in the upper tank of water supply end, which is used to filter possible impurities in the distilled water (filtered water, hereafter). At the right hand side of Fig. 4, details of the pedestal and top caps employed for saturated and unsaturated specimens are illustrated. For the unsaturated case, membrane filter (Nishimura et al. 2012, Wang et al. 2017c) is used for water drainage, and pore air can be controlled through another path in the top cap, where a hydrophobic filter is installed.

Four specimens were prepared for the permeability test as shown in Table 1 (specimen height: 100 mm, diameter: 50 mm). Saturated IOF-B specimen was formed by static compression method under the water content (w) of 12 % in a two-piece rigid mold. The specimen was saturated by the double vacuum method (Ampadu and Tatsuoka, 1993), and a B-value of more than 0.95 was obtained under 0 kPa back pressure. The specimen was consolidated first under a confining pressure of 50 kPa and then under 100 kPa. After each consolidation step, permeability was measured in several steps with different H_{su}. On the other hand, saturated Toyoura sand specimen was constituted by the air pluviation method and saturated by CO_2 flushing as well as application of back pressure of 200 kPa. Similar as IOF-B specimen, permeability was measured under different H_{su} after consolidation under 60 kPa and 100 kPa, respectively.

Unsaturated IOF-B specimen was prepared in the same way as the saturated IOF-B specimen, while extra water was added drop by drop from the top of the specimen until water drained from the bottom of the specimen. Such a specimen was cured overnight for a more uniform water distribution. The specimen was consolidated under a net stress of 100 kPa by allowing water drainage from the pedestal, and air drainage from the top cap. The average suction after consolidation was about 0.3 kPa and then the permeability was measured with a closed pore air path under a constant H_{su}. Unsaturated Toyoura sand specimen was prepared by compaction by 5 layers in a rigid mold. The initial w was 17.5 % and another 2.5 % of water was added after compaction and the specimen was cured for 2 hours thereafter. The specimen was consolidated under a net

stress of 100 kPa by only allowing pore air drainage from the top cap. Suction after consolidation was about 1.6 kPa and permeability test was conducted in the same way as the unsaturated IOF-B specimen. Note that during measurement of permeability, water inflow could not be monitored and the final *w* of Toyoura sand specimen increased from initially 20.0% to 21.2%, namely *w* increased 1.2% during the test.

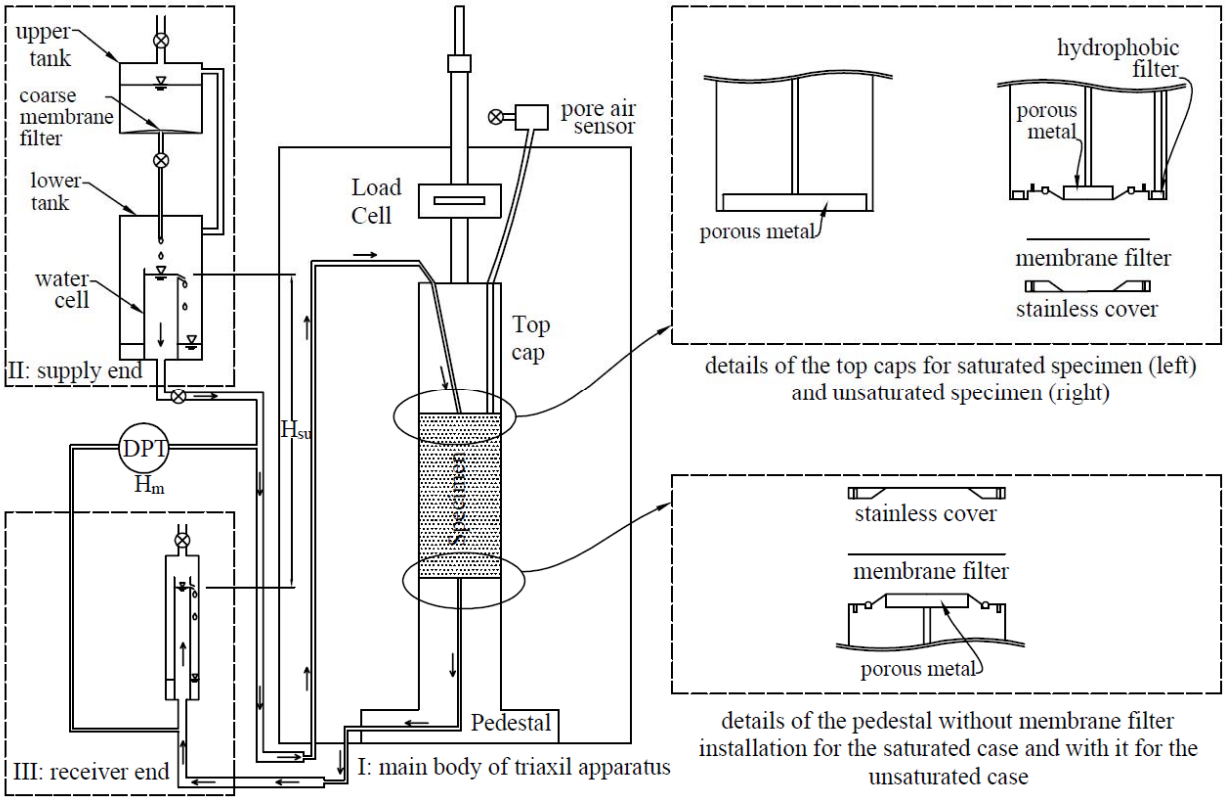

Fig. 4 Schematic illustration of the apparatus for permeability test

Table 1 Specimen conditions of permeability tests

Saturation conditions	Materials	σ_c (kPa)	ρ_d (Mg/m^3)	D_c or D_r (%)	S_r (%)	S (kPa)
Saturated tests	IOF-B	50→ 100	2.54→ 2.55	D_c: 91.3 → 91.7	100	-
	Toyoura sand	60→ 100	1.55→ 1.55	D_r: 78.1 → 78.4	100	-
Unsaturated tests	IOF-B	100	2.58	D_c: 92.7	84.3	1.6
	Toyoura sand	100	1.47	D_c: 51.8	69.8	0.3

Note: σ_c: confining pressure for saturated case and net stress for unsaturated case; ρ_d: dry densities after the consolidation; D_c, D_r: compaction degree and relative density after the consolidation; S_r: the values of unsaturated specimens were calculated according to the *w* at the end of test.

4 CALIBRATION OF SYSTEM HEAD LOSS AND FILTER CLOGGING ISSUE

To evaluate water head applied to the specimen (H_{sp}), system head loss (H_{sy}, i.e., water head consumed by the flow paths) needs to be first estimated. H_{sy} induced by filters (e.g., filter paper, porous stone) may be considered according to theoretical equation (e.g. Uno et al. 1990), while the rest caused by such as tube friction, changes of the flow direction at tube joints etc. can hardly be estimated theoretically. In this section, calibration tests to evaluate H_{sy} are introduced.

4.1 Calibration for saturated specimens

As the calibration test for the saturated specimens, a clean acrylic pipe and two filter papers were placed between the top cap and pedestal, H_m and water flow rate (*v*) were measured under difference H_{su}. Fig. 5 (a) shows *v* for the first seven steps with difference H_{su} (*v* is calculated in every 0.5 ml water discharge and H_m is indicated in the legend). It seems that *v* is almost constant at relative low H_m (e.g. steps 1-4), while it fluctuates somewhat at higher H_m. In addition, a very slight reduction of *v* associating water discharge is observed in each step. Steps 8 and 9 having a same H_{su} as step 5 were conducted immediately and about 12 hours later after step 7, respectively. Their *v* are plotted in Fig. 5 (b) together with that of step 5. It is revealed that magnitudes of *v* in steps 5 and 8 are very similar, while a slight reduction is observed in step 9, implying that duration of test may affect *v*.

Fig. 6 plots the relationship between H_m and *v* for steps 1-7 of the calibration test indicated by empty small circles, and larger circles are average value in each step. It seems that averaged H_m and *v* are approximately linearly related. Since the inner diameter of the acrylic pipe used in the calibration test was much larger compared to tubes in flow paths, head loose from

the acrylic pipe could be ignored. And H_{sy} in the permeability test could be estimated by this linear relationship (i.e. H_{sy}=317.9v) as far as the water path was kept unchanged. Then, H_{sp} in the permeability test was calculated by Equation (1). In addition, since the DPT position and drainage path connections were slightly different between permeability tests of IOF-B and Toyoura sand specimens, two calibration curves are shown in Fig. 6.

$$H_{sp} = H_m - H_{sy} \quad (1)$$

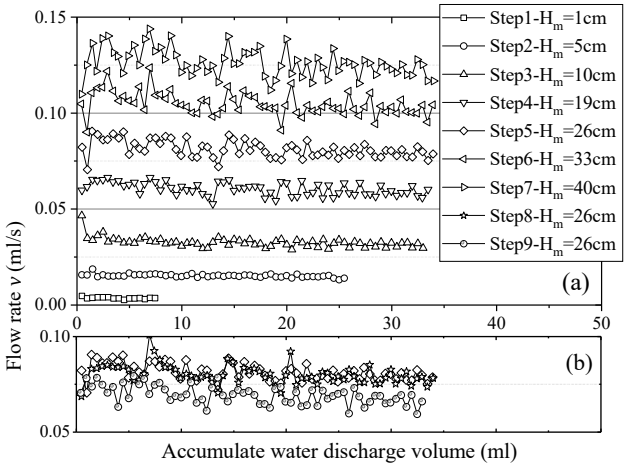

Fig. 5 Flow rate of calibration test for saturated case

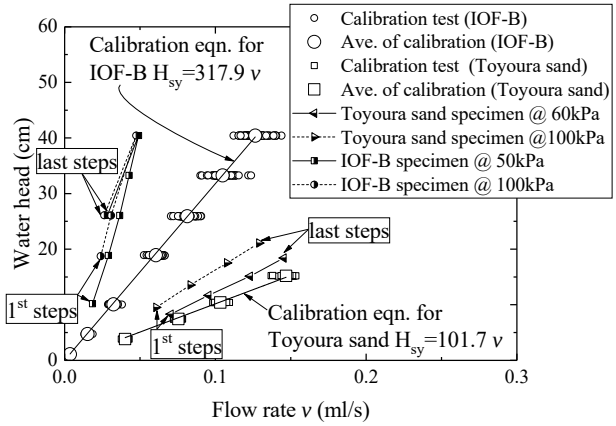

Fig. 6 Calibration for saturated specimens

4.2 Clogging issue and Calibration for unsaturated specimens

Before illustration of the calibration test for unsaturated specimens, the filter clogging issue is first explained based on tests conducted with the configuration shown in Fig. 7. These tests were to measure water head by DPT1 and flow rate (v) by DPT2 when water flowed through a membrane filter. Three tests were conducted with different water or procedures as shown in Table 2. In the second test, some fine contents of IOF-B were mixed to the water in the inner cell at the latter part of the virgin flow and in the third test, drainage was suspended overnight at the latter part of the second flow.

Measured water head and v are plotted in Fig. 8, where v is the rate for every 0.5 ml water discharge. It can be seen from Fig. 8 (a) that v of SF_1 becomes slower compared to that of VF_1 under the same water head, while v returns to the same level after changing to a new membrane filter (i.e. VF_1 versus VF_2). On the other hand, Fig. 8 (b) shows that v becomes faster by changing distilled water to filtered water (e.g. VF_1 versus VF_3) and v difference between VF and SF also becomes narrower by using filtered water. Further, apparently mixing IOF-B and extending test duration (i.e. latter parts of VF_2 and SF_3) also affects v. Fig. 8 and microscope observations (not shown) imply that filter clogging may occur due to flow of impurities together with water, which induces dependence of v on the accumulated volume of water discharge.

With the consideration of filter clogging issue, calibration tests for the unsaturated case were conducted with the following procedures. First, flow paths were sufficiently flushed and saturated by filtered water and initially saturated membrane filters were then immediately fixed to the top cap and pedestal. Thereafter the acrylic pipe was placed on the pedestal, filtered water was injected into the pipe from the top end of the pipe until water overflowed and the top cap was gently descended to the top end of the pipe ensuring that no air was trapped. Then water supply and receiver ends were adjusted to an appropriate positions. This condition was maintained for 3 hours to consider period of specimen consolidation and test preparation before permeability test. Lastly accumulated water discharge and v through membrane filters under the constant H_{su} were measured. The above procedures were repeated for other two H_{su} values.

In each calibration test, v was calculated for every 3 ml water discharge for simplification of calibration curves. The relationship between v and H_m is plotted in Fig. 9 indicated by empty symbols. It can be seen that v reduces continuously with the accumulated water discharge for all the three calibration tests and H_m in each calibration test slightly increases gradually due to the filter clogging. For estimation of H_{sy}, relationships between v and H_m were fitted by a hyperbolic function as indicated by dash lines in Fig. 9, by which H_{sp} of unsaturated specimens was estimated by Equation (1).

Table 2 Examination test for the filter clogging issue

Membrane filter No.	Types of Water	Procedures
1	Distilled water	Virgin flow (VF_1)→ Second flow (SF_1)
2	Distilled water	Virgin flow (VF_2) *addition of IOF-B at latter part of VF_2
3	Filtered water	Virgin flow (VF_3)→Second flow (SF_3) *suspension of water flow overnight at latter part of SF_3

Note: Virgin flow: water pass through a new membrane filter for the first time; Second flow: after refilling water to the original water level in the inner cell, water flow was repeated.

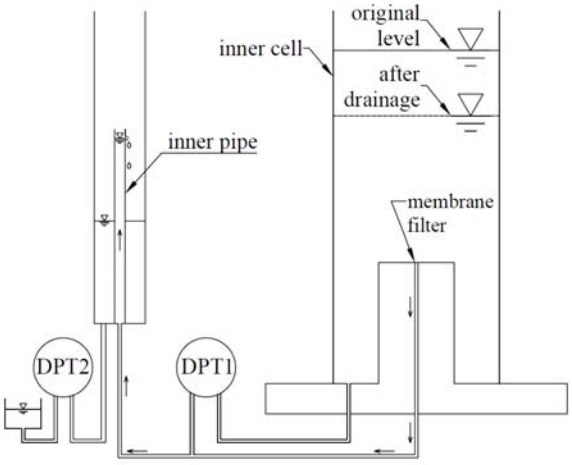

Fig. 7 Layout of testing apparatus for the filter clogging

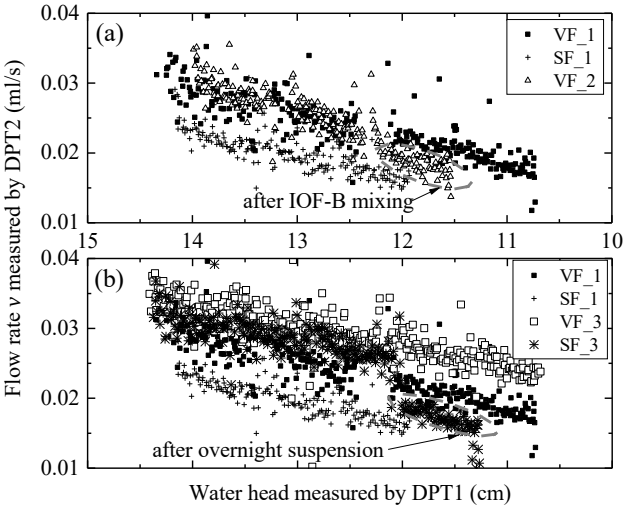

Fig. 8 Relationships between water head and flow rate in filter clogging examination test, (a) Tests 1 and 2; (b) Tests 1 and 3

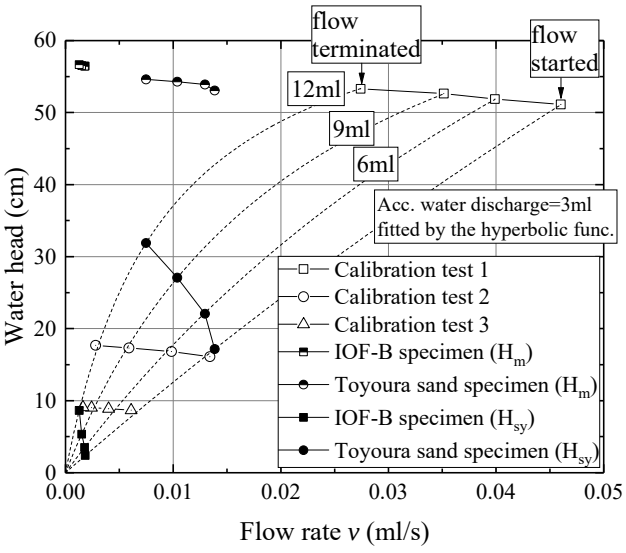

Fig. 9 Calibration test results of system for unsaturated specimens

5 PERMEABILITY TEST RESULTS AND DISCUSSIONS

5.1 Coefficient of permeability

It becomes straight forward to evaluate permeability of saturated and unsaturated specimens by knowing the H_{sy} and filter clogging issue discussed above. Fig. 10 shows typical evolution of v associated with water discharge of the saturated IOF-B specimen under different H_m. It can be seen that v reduces slightly with water discharge in each step, and it also reduces between steps even with the same H_m. These observations can also be seen slightly in the calibration tests as shown in Fig. 5 implying that filter clogging might occur during water flow through specimens. The relationship between averaged v and H_m in each step of two saturated tests are added to Fig. 6, from which it can be seen that when v is relatively small, H_{sy} consumes very large part of H_m (e.g. 1st step of Toyoura sand specimen) suggesting that the calibration is important in such a testing system.

Based on Darcy's law, hydraulic gradient (i) and coefficient of permeability (k) in each step of the two saturated specimens are calculated as shown in Fig. 11 (note that dimension changes of specimens due to consolidation are considered in calculation). It seems that in general k reduces accompanying an increase in i and has a trend of approaching to 10^{-5}m/s for IOF-B specimen and 10^{-4}m/s for Toyoura sand specimen. Carpenter and Stephenson (1986) conducted a series of test on a clay with k of an order of 10^{-10} m/s, by which it was found that k decreased (to about 1/3 at maximum) by increasing i from 50 to 300, while the reduction became ignorable by increase the diameter of the specimens. They attributed this reduction to consolidation effect when adjusting back pressure for desired i. While in this study since the volume change caused by consolidation is very small (see Table 1) and k of IOF-B specimen also reduces in the last steps as shown in Fig. 11, the reduction of k may be induced largely by the filter clogging issue which was not considered in the calibration tests.

For the two unsaturated specimens, the relationship between v (for every 3 ml water discharge) and accumulated water discharge is plotted in Fig. 12. It can be seen that v reduces associated with water discharge as expected, and the reduction magnitude is larger for Toyoura sand specimen. The relationships of H_m versus v of the two unsaturated specimens are added to Fig. 9, and H_{sy} is calculated accordingly as shown in the same figure, by which H_{sp} can be calculated. The coefficient of permeability k of the two specimens is plotted versus i in Fig. 13. It seems that k of unsaturated IOF-B and Toyoura sand specimens are about 2×10^{-7} m/s and 2×10^{-6} m/s, respectively. In addition, the apparent reduction of k with i is not observed as compared to the saturated case in Fig. 11, which may be attribute to a small v during flow of water.

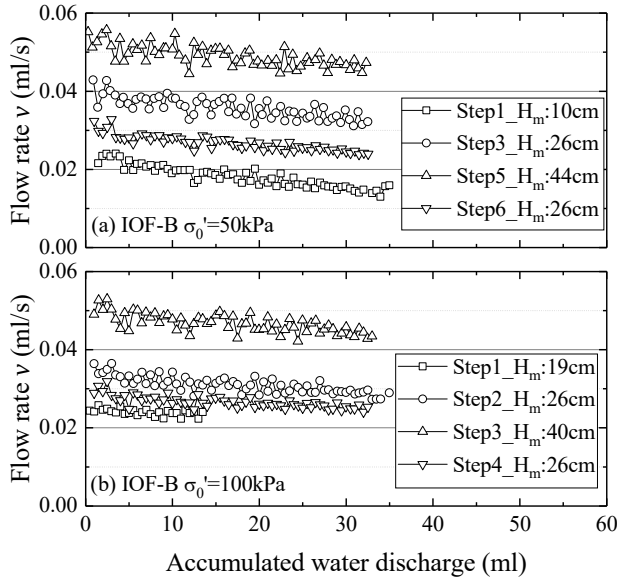

Fig. 10 Typical date of flow rate of in permeability test of unsaturated specimens (IOF-B)

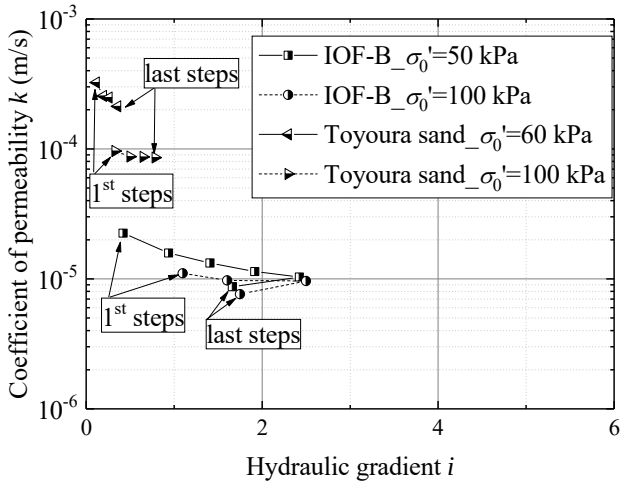

Fig. 11 Coefficient of permeability the two saturated specimens

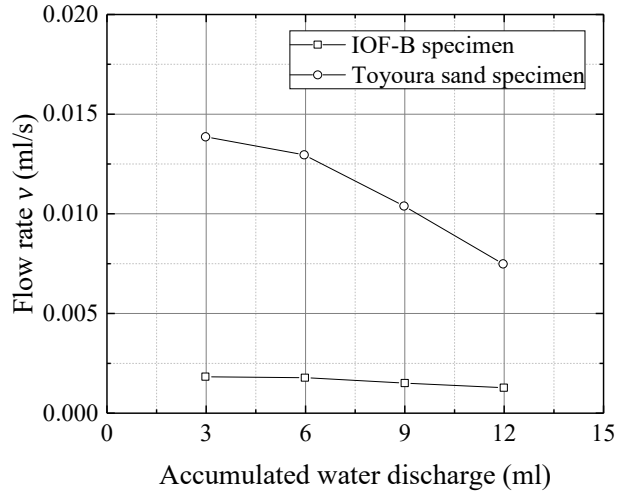

Fig. 12 Flow rate vs accumulated water discharge for unsatruated materials

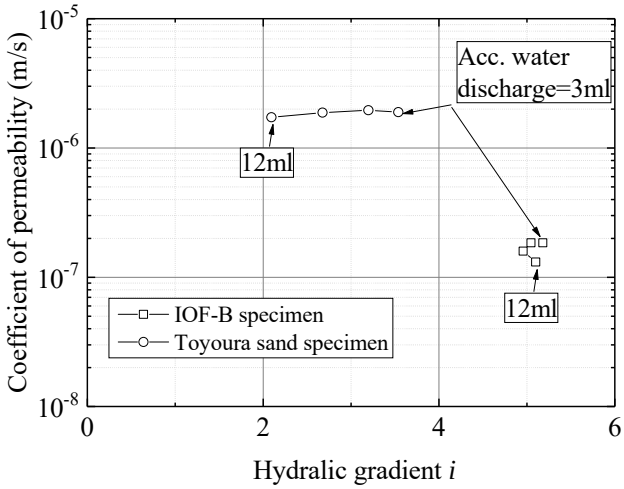

Fig. 13 Coefficient of permeability of two unsaturated specimens

5.2 Permeability of IOF-B in full range of S_r

For the seepage analysis of the IOF heap during maritime transportation, permeability of IOF-B in full range of S_r is necessary. In this section, k is estimated by VG model (Van Genuchten 1980) as shown by Equations (2) and (3).

$$k = k_s \Theta^{1/2} \left[1 \quad \left(1 \quad \Theta^{n/(n-1)} \right)^{1-1/n} \right]^2 \quad (2)$$

$$\Theta = \frac{\theta - \theta_r}{\theta_s - \theta_r} = \frac{1}{[1+|\alpha S|^n]^{1-1/n}} \quad (3)$$

where, θ_s, θ_r, k_s, k, α and n stand for saturated and residual volumetric water contents, coefficients of permeability for saturated and unsaturated conditions, two model parameters, respectively. S is suction. k_s $=1.0\times10^{-5}$m/s was set according to results in this study, and other parameters were determined as shown in Table 3 by fitting water retention curves (WRC) of IOF-B (Wang et al. 2014, see Fig. 14) with Equation (3) under three conditions. The first two conditions used drying and wetting processes of WRC in suction range 0.1-20kPa, respectively, and θ_r was set to be the value at S=20kPa. The third condition used drying process of WRC in full suction range by setting θ_r=0%.

In Fig. 15 the predicted k of the three cases is shown, where fitting curves of VG model (i.e. Equation 3) are indicated in the subfigure. It can be seen that the predicted k is roughly consistent with the measured k obtained in this study, though more measured data would be preferred for confirmation. Further, it can also be seen that k is significant different by assigning different θ_r (i.e. Case1 and Case 3), suggesting parameter sensitivity examination may be necessary in the seepage analysis.

5.3 Permeability of Toyoura sand in full range of S_r

To evaluate performance of the measurement system

employed in this study, a literature review on the coefficients of permeability of Toyoura sand was conducted and well documented data that were available to the authors were summarized in Table 4 and Fig. 16. It can be seen from Table 4 that the testing methods mostly used for laboratory measurement of permeability for unsaturated soils are included, such as steady state methods by employing Richards' type apparatus (Richards and Moore 1952) and triaxal apparatus (Ishikawa et al. 2010), and three unsteady state methods. The dry density values are mostly about 1.50 Mg/m^3, and hydraulic gradient values are in a range of 0.1-5 as shown by the available data. The filters used for the water drainage path were the ceramic disk, glass filter and membrane filter with coefficient of permeability in orders of 10^{-5}-10^{-9} m/s and thickness of 0.1-6 mm for available data. By reproducing these experimental results, three categories were made in Fig. 16, of which solid black data were measured by the steady state method and empty black data were measured by the unsteady state methods. The k-S_r in Kohno and Nishigaki (1981) and Kawanishi et al. (1987) were calculated from the θ-k relationship and the specimen dry density. However, in Kohno and Nishigaki (1981), ρ_d was said to be 1.50 Mg/m^3, by which the calculated data seem to shift to left hand side. On the other hand, θ_s of test specimen seemed to be about 0.3 from the other data in Kohno and Nishigaki (1981), which corresponds to a very large ρ_d=1.85 Mg/m^3. Thus Ko_IP and Ka_SS (ρ_d was arbitrary assigned) were grouped to gray solid marks.

First, for steady state method, it seems from Fig. 16 and Table 4 that permeability of used filters (k_{filter}) affect measured results very much. Data with k_{filter} of 2×10^{-6}-5×10^{-9}m/s distribute very close in S_r range of 60-100% as indicated by dash circle and the data in the study is lowest. On the other hand, k obtained with k_{filter} of 3×10^{-5} m/s distribute about one order higher. This results imply that filter selection in the steady state test may be crucial. Interestingly, the data regardless k_{filter} seems to converge in low S_r range (i.e.,S_r=20-60%). Secondly, for unsteady state methods, data by OI and IP methods (see notes under Table 4 for details of methods) seem to be consistent, and they are also consistent with steady state data. While data obtained by OS method distribute about 1-2 orders lower than OI and IP methods. In the OS method, relationship of water content change and time for one large step change of suction were measured, which may affect k_{filter}. For OI and IP methods, effects of k_{filter} might be less. With the above considerations, a distribution band is drawn indicated by the solid lines, which would be the most possible distribution area of k for Toyoura sand with density of about 1.5 Mg/m^3. Finally for results in this study, considering the variation of current data base, the data obtained may be still said to be reasonable.

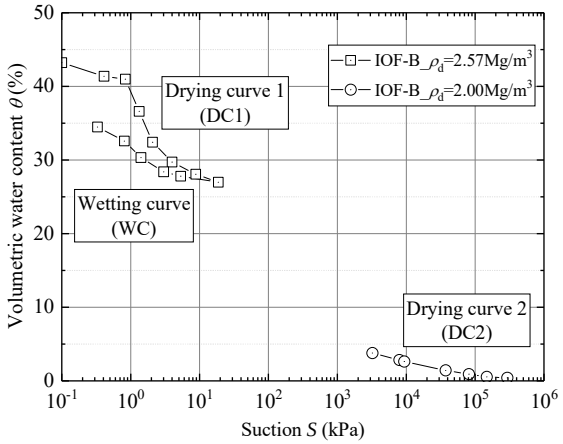

Fig. 14 SWCC of IOF-B (Wang et al. 2014)

Table 3 Parameters for VG model

Case	k_s (m/s)	θ_s (%)	θ_r (%)	a (kPa^{-1})	n
DC1	1.0×10^{-5}	42.1	27.0	0.75	2.79
WC		42.1	27.0	0.66	1.70
DC1+DC2		42.1	0	0.50	1.29

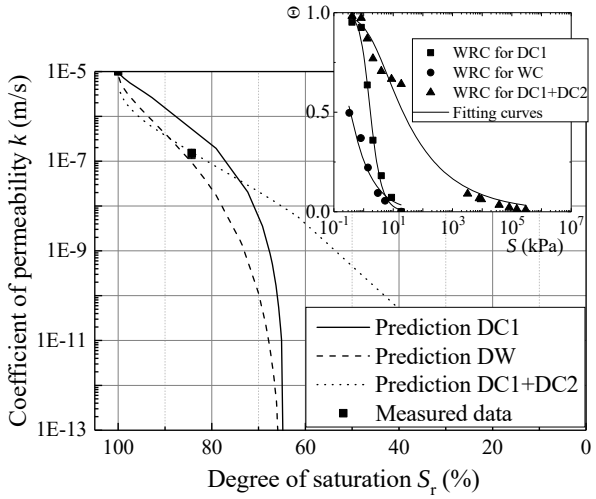

Fig. 15 Prediction of permeability of IOF-B in a full range of Sr

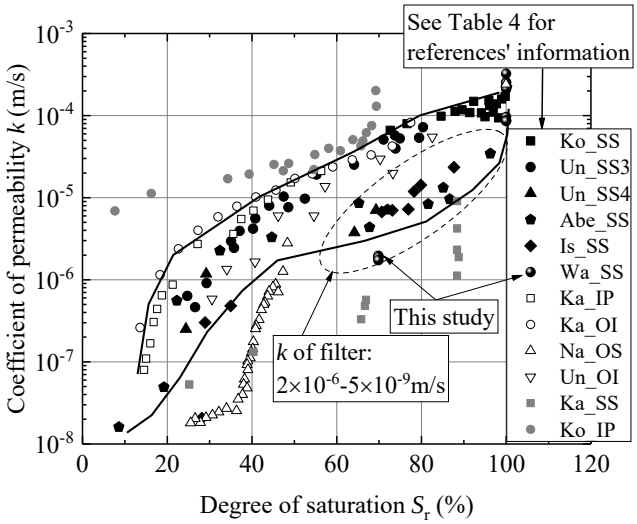

Fig. 16 Coefficient of permeability of Toyoura sand

Table 4 Literature review summary on parameter of Toyoura sand

References	Legend in Fig. 16	Method[1]	Dry density[2] (Mg/m^3)	Hydraulic gradient[3] i	Apparatus[4]	Specimen[5] dimension (mm)	Filter type	Filter thickness & permeability	Confining wall	Confining pressure (kPa)
Kohno & Nishigaki (1981)	Ko_IP	IP	1.50	NA	Acrylic cuboid	L:600 W:100 H:70	Porous plate	NA	Rigid	NA
Kohno & Nishigaki (1982)	Ko_SS	SS	1.57	NA	Richards' apparatus	NA	NA	NA	Rigid	NA
Nakagawa (1987)	Na_OS	OS	1.49*	NA	Triaxial apparatus	H:100 D:50	Ceramic disk	2 mm 2.71×10^{-5} m/s	Flexible	NA
Kawanishi et al. (1987)	Ka_SS	SS	1.48#	NA	Richards' apparatus	NA	NA	NA	Rigid	NA
	Ka_OI	OI	1.49*	NA	Acrylic pipe	H:100 D:50	NA	NA	Rigid	NA
	Ka_IP	IP	1.48*	NA	Acrylic pipe	H:1050 D:150	Metal mesh	NA	Rigid	NA
Uno et al. (1990)	Un_SS4	SS	1.50	NA	Richards' apparatus	H:40 D:60	Glass filter G4	6 mm $1.0\text{-}1.8\times10^{-7}$ m/s	Rigid	Unknown vertical loading
	Un_SS3	SS	1.50	0.3-4.6	Richards' apparatus	H:40 D:60	Glass filter G3	6 mm $2.3\text{-}2.8\times10^{-5}$ m/s	Rigid	
	Un_OI	OI	1.50-1.55	NA	NA	NA	ditto	ditto	NA	NA
Abe (1994)	Ab_SS	SS	1.49	0.5-1.5	Triaxial apparatus	H:20 D:50	Ceramic disk	3mm 2×10^{-6} m/s	Flexible	49
Ishikawa et al. (2010)	Is_SS	SS	1.60	0.5*	Triaxial apparatus	H:30 D:70	Membrane filter	NA 4.4×10^{-8} m/s	Flexible	49
This study	Wa_SS	SS	1.47	2.1-3.5	Triaxial apparatus	H:100 D:50	Membrane filter	0.14mm 5.2×10^{-9} m/s	Flexible	100

Note:

[1] Method: the methods to get coefficient of permeability, of which terminology in Klute (1972) is applied, SS: Steady state method which measure k by maintaining degree of saturation as constant condition, OS: one step method which measure the relationship between time and water drainage or absorption when suction of a specimen is changed in a relatively large step (k is assumed to be varying in this process), OI: Outflow and inflow method which measure the relationship between time and water drainage or absorption when suction of a specimen is changed in a relatively small step (k is assumed to be constant in this process) IP: Instantaneous profile method which measure the water content distribution along a specimen (usually very long) under a certain boundary condition (e.g. immerse one column end to water).

[2] values with * marks are calculated from void ratio by assuming G_s=2.65 and the value with # mark is an assigned value, by which volumetric water content q is converted to S_r in Fig. 16.

[3] Hydraulic gradient i is that applied to the two ends of specimens, the value with * mark is a value that is available from the reference, and NA stands for not available or not applicable.

[4] Richards' apparatus is basically similar apparatus similar to Richards and Moore (1952).

[5] H: specimen height, D: specimen diameter, L: specimen length, W: specimen width, NA: not available.

6 CONCLUSIONS

As part of testing program for evaluation of liquefaction potential of the heap of the iron ore fine (IOF) during maritime transportation, the study addressed results of permeability tests for saturated and unsaturated IOF-B and Toyoura sand. The following conclusions are obtained:

(1) A triaxial system was developed for permeability test for saturated and unsaturated sandy materials. This system could supply a constant water head, and the membrane filter technique was applied to the apparatus to acceleration of testing duration of the unsaturated specimen.

(2) From this study, k was about 1×10^{-5}m/s for saturated condition (S_r=100%) and 2×10^{-7} m/s for S_r=84% for IOF-B with dry density of 2.54-2.58 Mg/m^3. And k was about 1×10^{-4}m/s for saturated condition (S_r=100%) and 2×10^{-6} m/s for S_r=70% for Toyoura sand with dry density of 1.47 Mg/m^3.

(3) It was found that calibration of system head loss (H_{sy}) was very necessary and the filter clogging issue should be paid attention significantly for evaluation of k when the system did not directly measure water head different applied to a specimen.

(4) k in a full range of S_r for IOF-B were estimated based on the water retention properties, which shows that estimated data were close to the measurements. However, the number of measured data are very limited, further testing data of k for IOF-B or sensitivity check to k may be necessary in the seepage analysis of IOF heap.

(5) k in a full range of S_r for Toyoura sand that were well documented in the past studies were summarized. A general distribution band was drawn in k -S_r space, which implies the data in this study may be reasonable.

ACKNOWLEDGEMENTS

The first author would like to express great gratitude to Mr. T. Sato at Integrated Geotechnology Institute Ltd., Japan for his helps in the experimental work. The experimental work in this study was conducted in The University of Tokyo. This work was performed as a part of activities of the first author in the Research Institute of Sustainable Future Society, Waseda Research Institute for Science and Engineering, Waseda University.

REFERENCES

1) Abe, H. 1994. Experimental study on the estimation of mechanical properties for unsaturated soils. *Ph.D. Thesis, The University of Tokyo*, Japan (in Japanese).
2) Ampadu, S. K., and Tatsuoka, F. 1993. Effect of setting method on the behavior of clays in triaxial compression from saturated to undrained shear. *Soils and Foundations*, 33(2): 14-34.
3) Carpenter, G.W., and Stephenson R.W. (1986). Permeability testing in the triaxial cell. *Geotechnical Testing Journal*, Vol. 9, No. 1, pp: 3-9
4) Chen, W., Roberts, A., Katterfeld, A., and Wheeler, C. 2018. Modelling the stability of iron ore bulk cargoes during marine transport. *Powder Technology*, 326: 255–264.
5) IMSBC Code 2012. International Maritime Solid Bulk Cargoes Code. *IMO*.
6) IMO 2010a. Carriage of iron ore fines leading to marine casualties submitted by India. *IMO*, MSC 87/INF.13.
7) IMO 2010b. Carriage of iron ore fines that may liquefy. *IMO*, DSC.1/Circ.63.
8) IMO 2013a. Early implementation of draft amendments to the IMSBC Code related to the carriage and testing of iron ore fines. *IMO*, DSC.1/Circ.71.
9) IMO 2013b. Report of the correspondence group on transport of iron ore fines in bulk (part3). *IMO*, DSC18/INF. 9.
10) IMO 2013c. The technical working group (TWG) report#1 "Teams of reference.1". *IMO*, DSC18/INF. 10.
11) IMO 2013d. The technical working group (TWG) report#2 "Marine report". *IMO*, DSC18/INF. 11.
12) IMO 2013e. The technical working group (TWG) report#3 "Iron ore fine Proctor-Fagerberg test". IMO, DSC18/INF. 12.
13) IMO 2013f. The technical working group (TWG) report#4 "Reference tests". *IMO*, DSC18/INF. 13.
14) IMO 2015. Amendments to the international maritime solid bulk cargoes (IMSBC) code. *IMO*, MSC.393 (95).
15) Ishikawa, T., Tokoro, T., Ito, K. and Miura, S. 2010. Testing methods for hydro-mechanical characteristics of unsaturated soils subjected to one-dimensional freeze-thaw action. *Soils and Foundations*, 50 (3): 431-440.
16) JIS. 2009a. Test method for soil compaction using a rammer. JIS standard A1210. Japanese Industrial Standard Committee.
17) JIS. 2009b. Test method for minimum and maximum densities of sands. JIS standard A1224. Japanese Industrial Standard Committee.
18) Kawanishi, M., Tanaka, Y., Komada, H., and Siozaki, I. 1987. On the characteristics of moisture movement in unsaturated soils. *Proceeding in symposium on current researches of engineering properties of unsaturated soils*, pp. 245-252 (in Japanese).
19) Klute, A. 1972. The determination of the hydraulic conductivity and diffusivity of unsaturated soils. *Soil Science*, 133 (4): 264-276.
20) Kohno, I., and Nishigaki, M. 1981. An experimental study on characteristics of seepage through unsaturated sandy soil. *Proceedings of the Japan Society of Civil Engineers*, 1981 (307): 59-69 (in Japanese).
21) Kohno, I. and Nishigaki, M. 1982. Some aspects of laboratory permeability test. *Journal of the Japanese Society of Soil Mechanics and Foundation Engineering*, 22 (4): 181-190 (in Japanese).
22) Munro, M. C., and Mohajerani, A. 2018. Slope stability evaluation of iron ore fines during marine transport in bulk carriers. *Canadian Geotechnical Journal*, 55(2): 258–278.
23) Nakagawa, K. 1987. An experiment to determine the permeability of an unsaturated soil. *Proceeding in symposium on current researches of engineering properties of unsaturated soils*, pp. 253-257 (in Japanese)
24) Nishimura, T., Koseki, J., Fredlund, D.G., and Rahardjo, H. 2012. Microporous membrane technology for measurement of soil-water characteristic curve. *Geotechnical Testing Journal*, 35: 201-208.
25) Richards, L.A., and Moore, D.C. 1952. Influence of capillary conductivity and depth of wetting on moisture retention in soil. *Trans Am Geophys Union* 33(4), 531-540.
26) Roberts, S. E., Pettit, S. J., and Marlow, P. B. 2013. Casualties and loss of life in bulk carriers from 1980 to 2010. *Marine Policy*, 42: 223-235.
27) Van Genuchten, M. Th. 1980. A closed-form equation for predicting the hydraulic conductivity of unsaturated soils. *Soil Science Society of America Journal*, 44(5): 892-898.
28) Uno, T., Sato, T., Sigii, T., and Tsuge, H. 1990. Method of test for permeability of unsaturated sandy soil with controlled air pressure. *In Proc. of the Japan Society of Civil Engineers*, 1990(418): 115-124 (in Japanese).
29) Wang, H., Koseki, J., and Nishimura, T. 2014. SWCC measurement of two types of iron ores. *In Proceedings of the 6th International Conference on Unsaturated Soils*, Unsat2014, Sydney. pp. 973–979.
30) Wang, H., Koseki, J., Sato, T., Chiaro, G., and Tan Tian, J. 2016a. Effect of saturation on liquefaction resistance of iron ore fines and sandy soils. *Soils and Foundations*, 56(4): 732-744.
31) Wang, H., Koseki, J., Sato, T., and Miyashita, Y. 2016b. Geotechnical properties of a type of iron ore fines. *Japanese Geotechnical Society Special Publication*, 2(14): 541-546.
32) Wang, H., Sato, T., Koseki, J., Chiaro, G., and Tan Tian, J. 2016c. A system to measure volume change of unsaturated soils in undrained cyclic triaxial tests. *Geotechnical Testing Journal*, 39(4): 532-542.
33) Wang, H., Koseki, J., and Cai., F. 2017a. Numerical evaluation of liquefaction potential of the heap of iron ore fines during maritime transportation. *In Proceedings of the 19th International Conference of Soil Mechanism and geotechnical Engineering*, Seoul, Korea, pp.1447-1450.
34) Wang, H., Koseki, J., and Sato, T. 2017b. p-constant Condition Applied to Undrained Cyclic Triaxial Test of Unsaturated Soils. *Geotechnical Testing Journal*, 40(4): 710-718.
35) Wang, H., Koseki, J. Nishimura, T., and Miyashita, Y. 2017c. Membrane filter properties and application of the filter to undrained cyclic triaxial test of unsaturated materials. *Canadian Geotechnical Journal*, 54(8): 1196-1202.
36) Wang, H., Koseki, J., Cai, F., and Nishimura, T. 2018. Undrained monotonic triaxial loading behaviors of a type of iron ore fines. *Canadian Geotechnical Journal*, 55 (9): 1349-1357.